International Journal of Engineering Research & Technology (IJERT)
ISSN: 2278-0181
Vol. 14, Issue 09, RTMSE-2026

Surface Roughness and Morphology Evolution in Wire EDM of Nickel-Based Superalloys: A Critical Review

Gurnam Singh[1], Neel Kanth Grover[1] and Vivek Aggarwal[1]
[1] Department of Mechanical Engineering, IK Gujral Punjab Technical University, Kapurthala, Punjab, India
Correspondence to: Gurnam Singh / gurnamsingh@sbsstc.ac.in

***Abstract*— Wire Electrical Discharge Machining (WEDM) is widely used for precision machining of nickel-based superalloys for aerospace and high-temperature applications; however, the process inherently alters surface integrity because of intense thermo-electrical interactions. This review critically synthesizes the published literature on surface roughness and morphology evolution in WEDM-processed nickel-based superalloys. It identifies discharge energy—primarily governed by pulse-on time, peak current, gap voltage, and machining strategy—as the dominant factor controlling crater formation, molten material redeposition, surface roughness, and morphology evolution. Reported surface roughness spans a wide range, from above 7 µm during aggressive rough cutting to about 0.16–0.6 µm under optimized low-energy trim-cut conditions. Rough cutting generally produces irregular, debris-laden surfaces, whereas successive trim cuts significantly improve surface finish and morphological uniformity. Material-dependent responses are also evident, with Inconel 625 and Inconel 718 generally exhibiting smoother surfaces than Nimonic-based alloys and B1914 under comparable conditions. The review emphasizes that integrated evaluation of surface roughness and morphology is essential for ensuring reliable functional performance of WEDM-processed superalloy components.**

Keywords - WEDM; Nickel-based superalloys; Surface roughness; Surface morphology; Discharge energy; Surface integrity

I. INTRODUCTION

Wire Electrical Discharge Machining is a widely used non-conventional machining process for fabricating components from difficult-to-cut materials, particularly Ni-based superalloys employed in aerospace and high-temperature applications. Conventional machining of these alloys is limited by severe tool wear, high cutting forces, and dimensional inaccuracy. In contrast, WEDM utilizes controlled thermo-electric erosion without mechanical contact, enabling precise machining of complex geometries with minimal mechanical stresses.

As illustrated in Fig. 1, WEDM employs a continuously fed wire electrode and repetitive electrical discharges across a narrow dielectric-filled spark gap. The dielectric flushing system removes molten debris and maintains process stability [1]. However, the intense localized heating and rapid quenching inherent to WEDM introduce surface integrity concerns, requiring careful control of electrical parameters and flushing conditions.

Previous studies indicate that surface integrity is governed primarily by discharge energy and machining strategy. Antar et al. [2] showed that rough cutting generates irregular, debris-laden surfaces, while successive trim cuts significantly improve finish and morphology. Li et al. [3] reported progressive surface enhancement in Inconel-718 through multi-trim WEDM with reduced discharge energy. Similarly, Goswami and Kumar [4] identified T_{on} and I_p as dominant factors influencing crater formation, roughness, and defect evolution.

Building on these insights, the following review synthesizes existing studies to identify governing trends, material-dependent responses, and research gaps related to surface roughness and morphology in WEDM of nickel-based superalloys.

II. LITERATURE REVIEW

WEDM has been widely investigated for Ni-based and related superalloys, where surface roughness and surface morphology are recognized as primary indicators of surface integrity. Across alloy systems and machining strategies, the literature consistently identifies discharge energy, governed mainly by T_{on}, I_p, duty factor, and discharge frequency, as the dominant parameter controlling crater formation, material redeposition, and defect evolution.

Early experimental studies established that increasing discharge energy enlarges crater size, intensifies molten material redeposition, and promotes the formation of debris-laden recast layers. Sharma et al. [5] demonstrated for Inconel-706 that surface roughness increases monotonically with discharge energy due to deeper craters and resolidified debris, while smoother surfaces are obtained at low T_{on} and high SV through improved flushing. Notably, surface microcracks were absent, highlighting the mitigating role of alloy toughness. Similar discharge-energy-controlled trends were reported for Nimonic-80A by Goswami and Kumar [6], who showed that higher T_{on} and I_p produce crater-dominated, debris-rich surfaces, whereas increased pulse-off time reduces surface damage by limiting discharge concentration.

To rationalize such observations, Atzeni et al. [7] introduced a nominal discharge energy per unit length for Inconel-718, providing a physically meaningful descriptor linking electrical input to surface outcomes. Their results showed that roughing conditions can yield Ra values as high as ~7.6 µm, associated with dense and irregular crater fields,

International Journal of Engineering Research & Technology (IJERT)
ISSN: 2278-0181
Vol. 14, Issue 09, RTMSE-2026

whereas finishing operations reduce Ra to ~1.7–2.3 µm by suppressing melting and redeposition. This energy-based framework explains why multi-stage machining strategies are consistently effective in stabilizing both surface roughness and morphology across alloys.

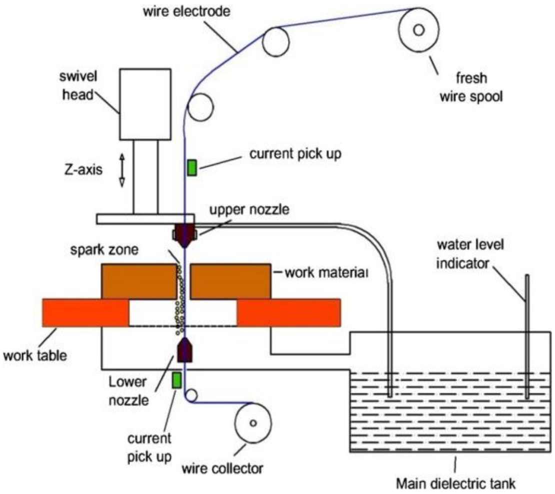

Fig. 1. WEDM setup showing the wire electrode path, spark zone, dielectric flushing system, and key machine components [1].

Beyond electrical parameters, several studies highlight the influence of wire material and configuration on discharge stability and flushing efficiency. Sharma et al. [8] reported that hard brass wire produces lower surface roughness than Zn-coated wire during WEDM of Inconel-706 due to improved discharge stability and reduced vibration, whereas zinc-coated wire, despite enhancing cutting rate, increases crater size and debris accumulation. Sharma et al. [9] further showed that larger wire diameter increases Ra by ~8% due to reduced flushing efficiency, resulting in defect-dense morphologies at high energy.

Material-specific responses modulate these general trends. For Udimet-L605 (Haynes-25), Sharma et al. [10] observed overlapping craters, molten globules, and micro-voids at high discharge energy, while low-energy regimes yielded smoother surfaces with microcracks confined to the recast layer. Similar energy-dependent morphology was reported for Nimonic-90 by Kumar et al. [11]. Mandal et al. [12] demonstrated that rough cutting of Nimonic-C263 produces severely irregular “coral-reef” morphology, and meaningful integrity improvement requires finish cutting and post-processing.

Fatigue-oriented investigations reveal the functional consequences of morphology. Chen et al. [13] showed that craters, voids, and microcracks in Inconel-718 act as fatigue crack initiation sites, while Shabgard et al. [14] linked microcrack density in Inconel-617 directly to discharge energy and thermal stress evolution, emphasizing that morphology governs service performance beyond roughness alone.

Optimization studies reaffirm discharge energy dominance but expose methodological gaps. Sharma et al. [15] confirmed pulse-on time as the governing factor in Inconel-706. Garg et al. [16] noted that most WEDM research prioritizes statistical optimization of Ra, with limited mechanistic analysis of morphology. Shandilya et al. [17] and Bisaria and Shandilya [18] emphasized integrating roughness, morphology, and compositional assessment for comprehensive surface integrity evaluation.

Comparative investigations reinforce the universality of energy-driven degradation with alloy-dependent sensitivity. Sreenivasa Rao and Venkaiah [19], Gowthamana and Jeyakumarb [20], and Joy et al. [21] demonstrated monotonic roughness–energy relationships across Inconel-690 and Hastelloy-X. Studies on Waspaloy, Inconel-718, Inconel-939, and other advanced alloys [22–28] consistently showed that stable, low-energy machining produces smoother, defect-limited surfaces. Benchmarking studies [29–34] further confirmed pulse-on time, voltage, and arc-on time as dominant parameters across wrought and additively manufactured superalloys.

Overall, although surface roughness and morphology are closely related, they capture different aspects of surface integrity. Ra reflects average crater geometry governed by discharge energy, whereas morphology encompasses crater overlap, debris adhesion, and microcrack distribution—features that more directly influence fatigue and functional performance. The following section therefore presents a focused discussion on surface roughness and surface morphology based on these synthesized insights.

III. SURFACE ROUGHNESS

Surface roughness in WEDM-processed superalloys is primarily governed by discharge energy, controlled through T_{on}, I_p, duty factor, and machining sequence. Increasing discharge energy produces larger and deeper craters, intensified molten redeposition, and unstable sparking, resulting in higher Ra. SEM and 3D topography analyses of alloys such as Inconel 718, Inconel 706, and Udimet-L605 confirm that roughness trends closely follow crater density and debris accumulation.

Machining strategy strongly influences surface finish. Rough cutting generates irregular, crater-dominated surfaces, whereas successive trim cuts reduce discharge energy and stabilize sparking, progressively lowering Ra. For example, Inconel 718 shows a reduction from ~2.01 µm (rough cut) to ~0.43 µm (final trim), while Udimet 720 and Ti-6246 achieve ~0.6 µm after the second trim pass. Across Nimonic, Inconel, and related alloys, optimized low-energy conditions yield Ra values as low as ~0.16 µm.

Electrical parameters further modulate roughness. Higher T_{on} and I_p increase Ra, while higher T_{off}, servo voltage, and spark gap voltage improve finish by enhancing flushing and reducing discharge intensity. Energy-normalized analyses indicate Ra up to ~7.6 µm under aggressive roughing, decreasing to ~1.7–2.3 µm during finishing. Pulse-on time is consistently the dominant factor, contributing 40–80% of total roughness variation.

Material and process effects are evident. Hard brass wire generally yields lower Ra than zinc-coated wire, and larger wire diameters increase roughness (~8%) due to reduced

International Journal of Engineering Research & Technology (IJERT)
ISSN: 2278-0181
Vol. 14, Issue 09, RTMSE-2026

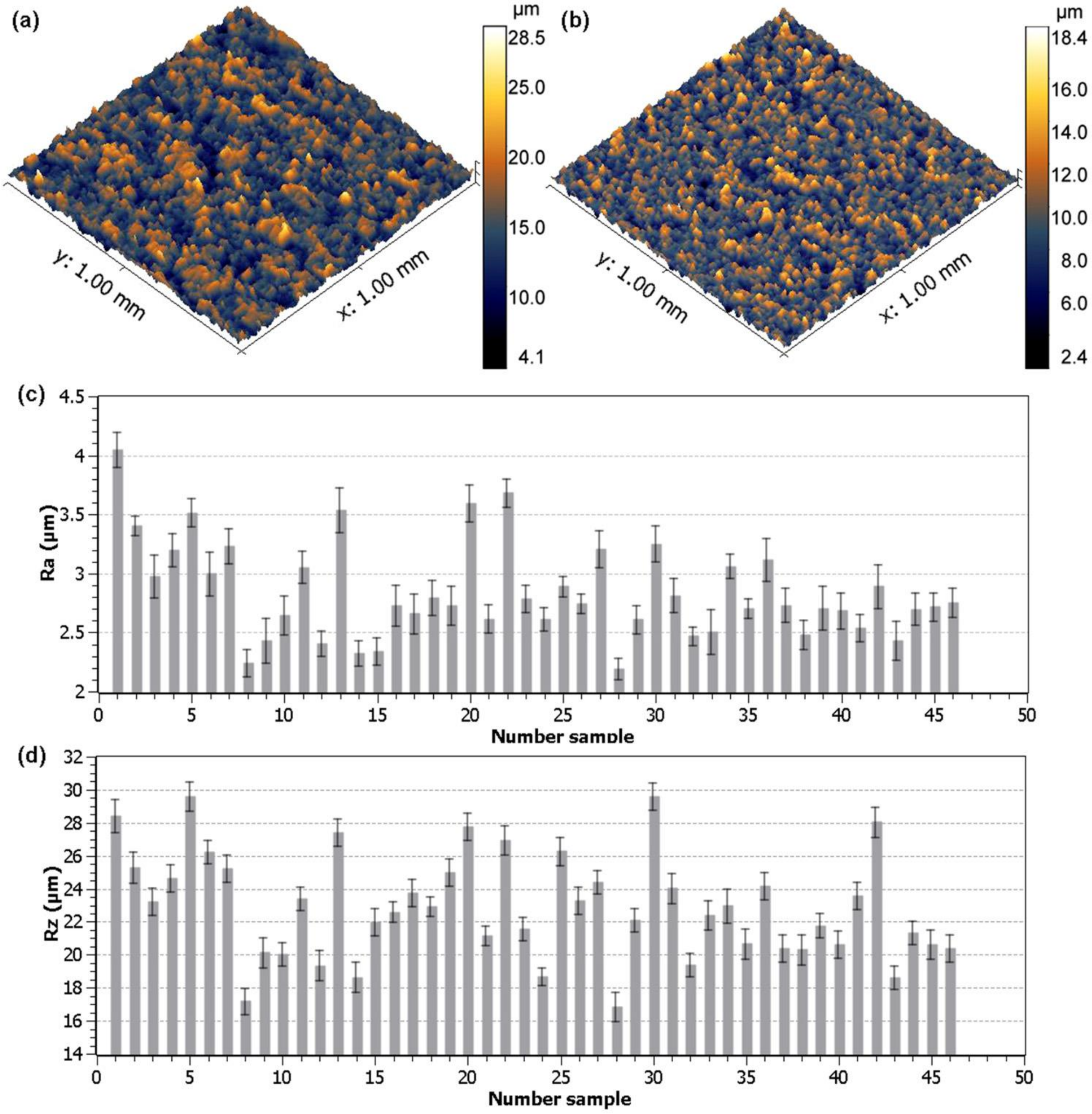

Fig. 2. (a) Three-dimensional (3D) relief of sample 1, (b) 3D relief of sample 28, (c) the evaluated parameter Ra for all machined samples and (d) the evaluated parameter Rz for all machined samples [29].

flushing efficiency. Additively manufactured alloys (e.g., Inconel 939, SLM-Udimet 720) show heightened energy sensitivity. Comparative studies indicate that Inconel 625 and B1914 achieve relatively lower Ra under optimized conditions, whereas Nimonic-C263 and MONEL K-500 tend to exhibit higher roughness.

Importantly, roughness alone does not fully capture surface integrity. High-Ra surfaces with craters, globules, and micro-voids act as fatigue crack initiation sites, while post-processing can reduce Ra to ~0.024 µm. Fig. 2 exemplifies the energy–roughness relationship in B1914, where minimum roughness (Ra ≈ 2.18 µm) occurs under low T_{on} and current, demonstrating the trade-off between cutting speed and surface quality. Table I summarizes reported Ra ranges and corresponding morphological features across nickel-based superalloys, reinforcing the dominant role of discharge energy in roughness evolution.

IV. SURFACE MORPHOLOGY

Surface morphology of WEDM-machined high-temperature superalloys is characterized by overlapping discharge craters, resolidified globules, surface cavities, debris adhesion, and recast-layer coverage, all strongly governed by discharge energy. SEM analyses of alloys such as Inconel 718, Inconel 706, Udimet-L605, and Nimonic grades consistently show that high discharge energy produces deep, irregular craters and extensive debris redeposition, whereas reduced energy and multi-pass strategies yield smoother, more uniform surfaces.

A distinct morphological transition with machining sequence is widely observed. Rough-cut conditions generate

International Journal of Engineering Research & Technology (IJERT)
ISSN: 2278-0181
Vol. 14, Issue 09, RTMSE-2026

irregular "coral-reef" structures with trapped voids and discontinuous recast layers, while successive trim cuts suppress crater overlap and debris accumulation, producing isotropic textures with shallow craters and minimal defects. In alloys such as Inconel 718 and Udimet 720, trim cuts significantly improve morphological uniformity, with microcracks often absent and thermal damage confined to the near-surface region.

TABLE 1. SUMMARY OF SURFACE ROUGHNESS (RA/RZ), CHARACTERISTIC SURFACE MORPHOLOGY, AND DOMINANT WEDM PARAMETER RANGES FOR NICKEL-BASED SUPERALLOYS REPORTED IN THE LITERATURE

Material & Corresponding Author(s)	Key Input Parameters (Optimized Ranges)	Surface Roughness (Ra, Rz)	Surface Morphology
B1914, Mouralová *et al.*	Ton: 4–8 µs; Toff: 6–12 µs; Ip: 4–8 A; Wire feed: 6–10 m/min	Ra ≈ 2.18 µm, Rz ≈ 16.86 µm	Cratered surface with molten globules and resolidified debris; smoother morphology at low energy
Inconel 718, Alkahlan *et al.*; Reolon *et al.*; Abhilash & Chakradhar	Ton: 0.6–1.2 µs; Toff: 8–14 µs; Ip: 3–7 A; GV: 40–60 V	Ra ≈ 1.7–3.5 µm	Shallow craters, micro-globules; microcracks under unstable machining
Inconel 690, Sreenivasa Rao & Venkaiah	Ton: 6–10 µs; Toff: 6–10 µs; Ip: 6–10 A	Ra ≈ 0.28–3.25 µm	Thick porous recast layer with microvoids and resolidified droplets
Inconel 706, Sharma *et al*	Ton: 4–8 µs; Toff: 6–12 µs; Wire Ø: 0.18–0.25 mm	Ra ≈ 1.8–3.8 µm	Uniform crater distribution; largely crack-free at optimized parameters
Inconel 625, Polzer *et al.*; Biswas *et al.*	Ton: 0.5–1.0 µs; Toff: 10–14 µs; Ip: 3–6 A	Ra ≈ 1.6–2.9 µm	Smooth morphology with shallow craters and limited debris
Inconel 738, Devanathan *et al.*	Ton: 4–8 µs; Toff: 6–12 µs; Voltage: 40–70 V	Ra ≈ 1.64–2.72 µm	Roughened cratered surface at high voltage; smoother under optimized settings
Nimonic C-263, Mandal *et al.*	Rough: Ton 6–10 µs; Trim: Ton 1–3 µs	Ra ≈ 2.13 µm → 0.024 µm	Thick oxidized recast layer; post-processing yields smooth, damage-free surface
Nimonic 90, Kumar *et al.*	Ton: 3–6 µs; Toff: 8–12 µs	Ra decreases at low Ton	Fine craters with minimal microcracking
Hastelloy X, Joy *et al.*	Ton: 4–8 µs; Cutting angle: 0°–60°	Qualitative	Molten globules and craters; improved uniformity at higher angles
Udimet-L605, Sharma *et al.*	Ton: 6–10 µs; Ip: 6–10 A	Ra increases with Ton	Rough morphology with heavy resolidified deposits
Waspaloy, Srinivasan *et al.*	Duty factor: 0.4–0.8; Ip: 6–12 A	Ra increases with duty factor	Dense globules and carbide-rich resolidified layer
MONEL K-500, Karthikeyan *et al.*	Ton: 4–8 µs; Toff: 5–10 µs; GV: 40–60 V	Ra ≈ 3.6–5.4 µm	Large craters and surface cracks at high Ton

Discharge energy remains the dominant driver of defect formation. High pulse-on time and peak current promote molten pool instability, leading to globules, micro-voids, and localized cracking, typically restricted to the recast layer. In contrast, low-energy regimes produce compact surfaces with reduced crater depth and defect density, and subsurface microstructural alteration is rarely reported.

Material-dependent responses are evident. Alloys with higher thermal conductivity and toughness (e.g., Inconel 625 and Inconel 718) generally exhibit smoother morphologies under comparable conditions, whereas Nimonic C-263 and B1914 show greater sensitivity to discharge energy. Additively manufactured superalloys (e.g., Inconel 939, SLM-Udimet 720) display enhanced morphological variability due to microstructural heterogeneity. Wire material and machining stability further influence crater geometry and debris adhesion, with hard brass wire and stable sparking producing more refined surface textures.

Overall, surface morphology provides a more comprehensive indicator of surface integrity than roughness alone, as crater overlap, debris adhesion, and microcrack density directly influence fatigue performance and service reliability.

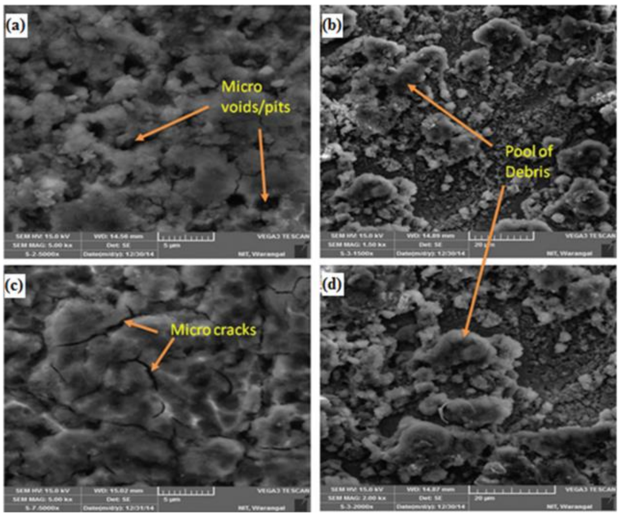

Fig. 3. SEM micrographs illustrating typical surface defects in WEDM: (a) micro-voids/pits, (b) and (d) resolidified debris pools, and (c) micro-cracks formed due to thermal stresses during machining [19].

As a representative example, Fig. 3 illustrates typical WEDM-induced surface defects—micro-voids/pits, debris pools, and micro-cracks—formed under high discharge energy conditions, where intense localized melting and insufficient flushing promote debris redeposition and thermal stress accumulation. The material-dependent evolution of crater morphology, debris adhesion, and recast-layer continuity discussed above is systematically summarized in Table 1, which correlates surface roughness ranges with characteristic morphological features across nickel-based superalloys, highlighting the dominant role of discharge energy in governing both roughness and surface morphology.

Fig. 4 presents a color-coded heat-map comparing surface roughness and surface morphology severity for WEDM-processed nickel-based superalloys. The severity index (1 = low/better integrity; 5 = high/poorer integrity) synthesizes reported Ra trends and qualitative morphological features (crater density, globules, micro-cracks, debris adhesion). Alloys such as Inconel 625 and Inconel 718 cluster in the low-severity region, indicating smoother surfaces and more uniform morphology under optimized parameters. B1914 and Nimonic 90 show moderate severity, reflecting stronger sensitivity to discharge energy. In contrast, Nimonic C-263, Udimet-L605, and Waspaloy exhibit higher morphological severity despite acceptable roughness in some cases, highlighting recast-layer dominance. MONEL K-500 shows the highest roughness severity, consistent with pronounced cratering and surface cracking at elevated pulse energy. Overall, the heat-map visually emphasizes material-dependent trade-offs between achievable surface finish and morphological integrity in WEDM.

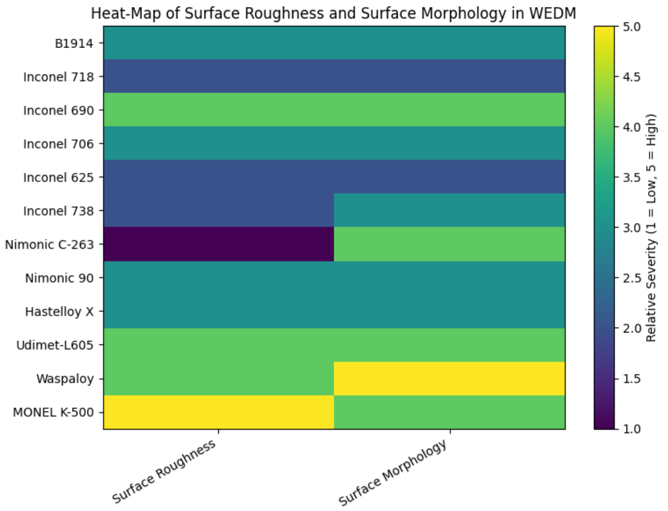

Fig. 4. Color-coded heat-map comparison of surface roughness and surface morphology for WEDM-processed nickel-based superalloys, where lower severity values indicate improved surface integrity.

V. FINDINGS FROM PRESENT RESEARCH STUDY

Following are the key findings derived from the comprehensive literature survey on WEDM of nickel-based superalloys:

- Very limited research has been reported on newly evolving nickel-based superalloys, such as Haynes grades and René N5, despite their extensive use in advanced aero-engine hot-section components.
- Limited studies address WEDM of additively manufactured nickel-based superalloys, even though AM components are increasingly adopted in aerospace applications.

VI. CONCLUSIONS

- Discharge energy, governed primarily by pulse-on time and peak current, is the dominant factor controlling surface roughness and morphology evolution in WEDM of nickel-based superalloys.
- Surface roughness decreases from >7 µm under aggressive roughing to ~0.16–0.6 µm under optimized trim-cut conditions, confirming that controlled low-energy and multi-pass strategies are essential for minimizing crater formation and molten redeposition while achieving aerospace-grade surface quality.
- Alloys such as Inconel 625 and Inconel 718 generally exhibit smoother surfaces and improved morphological stability under optimized conditions, whereas Nimonic-based alloys and B1914 show greater sensitivity to discharge energy, resulting in thicker recast features, deeper crater formation, and higher roughness under comparable machining regimes.
- Microcracks, when present, remain largely confined to the near-surface resolidified layer, indicating localized thermal damage rather than bulk material degradation.
- Wire characteristics, flushing stability, and alloy thermophysical properties modulate surface response; brass wire, particularly hard brass, remains the most widely adopted electrode due to its discharge stability and balanced performance.
- Integrated evaluation of discharge parameters, roughness, and morphological descriptors is essential for reliable optimization of WEDM in high-temperature aerospace applications.

DECLARATION OF INTEREST

The authors declare that there is no conflict of interest in publishing this manuscript.

ACKNOWLEDGEMENT

The authors gratefully acknowledge the support of the Department of Mechanical Engineering, I.K. Gujral Punjab Technical University, Kapurthala, and sincerely thank the researchers whose published works have significantly contributed to the development of this comprehensive review on WEDM of nickel-based superalloys.

REFERENCES

[1] N. Kuruvila and R. H V., "Parametric Influence and Optimization of Wire EDM of Hot Die Steel," *Machining Science and Technology*, vol. 15, no. 1, pp. 47–75, Mar. 2011, doi: 10.1080/10910344.2011.557966.

[2] M. T. Antar, S. L. Soo, D. K. Aspinwall, D. Jones, and R. Perez, "Productivity and workpiece surface integrity when WEDM aerospace alloys using coated wires," *Procedia Engineering*, vol. 19, pp. 3–8, Jan. 2011, doi: 10.1016/j.proeng.2011.11.071.

[3] L. Li, X. T. Wei, and Z. Y. Li, "Surface integrity evolution and machining efficiency analysis of W-EDM of nickel-based alloy," *Applied Surface Science*, vol. 313, pp. 138–143, Jun. 2014, doi: 10.1016/j.apsusc.2014.05.165.

[4] A. Goswami and J. Kumar, "Optimization in wire-cut EDM of Nimonic-80A using Taguchi's approach and utility concept," *Engineering Science and Technology an International Journal*, vol. 17, no. 4, pp. 236–246, Sep. 2014, doi: 10.1016/j.jestch.2014.07.001.

[5] P. Sharma, D. Chakradhar, and S. Narendranath, "Evaluation of WEDM performance characteristics of Inconel 706 for turbine disk application," *Materials & Design*, vol. 88, pp. 558–566, Sep. 2015, doi: 10.1016/j.matdes.2015.09.036.

[6] A. Goswami and J. Kumar, "Surface topography and kerf study of Nimonic 80A using Wire-Cut EDM," *Materials Science Forum*, vol. 808, pp. 35–41, Dec. 2014, doi: 10.4028/www.scientific.net/msf.808.35.

[7] E. Atzeni, E. Bassoli, A. Gatto, L. Iuliano, P. Minetola, and A. Salmi, "Surface and sub surface evaluation in Coated-Wire Electrical Discharge Machining (WEDM) of INCONEL® Alloy 718," *Procedia CIRP*, vol. 33, pp. 388–393, Jan. 2015, doi: 10.1016/j.procir.2015.06.089.

[8] P. Sharma, D. Chakradhar, and S. Narendranath, "Effect of wire material on productivity and surface integrity of WEDM-Processed Inconel 706 for aircraft application," *Journal of Materials Engineering and Performance*, vol. 25, no. 9, pp. 3672–3681, Jul. 2016, doi: 10.1007/s11665-016-2216-z.

[9] P. Sharma, D. Chakradhar, and S. Narendranath, "Effect of wire diameter on surface integrity of wire electrical discharge machined Inconel 706 for gas turbine application," *Journal of Manufacturing Processes*, vol. 24, pp. 170–178, Sep. 2016, doi: 10.1016/j.jmapro.2016.09.001.

[10] S. S. Nain, D. Garg, and S. Kumar, "Modeling and optimization of process variables of wire-cut electric discharge machining of super alloy Udimet-L605," *Engineering Science and Technology an International Journal*, vol. 20, no. 1, pp. 247–264, Oct. 2016, doi: 10.1016/j.jestch.2016.09.023.

[11] V. Kumar, K. K. Jangra, V. Kumar, and N. Sharma, "WEDM of nickel based aerospace alloy: optimization of process parameters and modelling," *International Journal on Interactive Design and Manufacturing (IJIDeM)*, vol. 11, no. 4, pp. 917–929, Jan. 2016, doi: 10.1007/s12008-016-0298-3.

[12] A. Mandal, A. R. Dixit, S. Chattopadhyaya, A. Paramanik, S. Hloch, and G. Królczyk, "Improvement of surface integrity of Nimonic C 263 super alloy produced by WEDM through various post-processing techniques," *The International Journal of Advanced Manufacturing Technology*, vol. 93, no. 1–4, pp. 433–443, Jan. 2017, doi: 10.1007/s00170-017-9993-x.

[13] Z. Chen, J. Moverare, R. L. Peng, and S. Johansson, "Surface integrity and fatigue performance of Inconel 718 in wire electrical discharge machining," *Procedia CIRP*, vol. 45, pp. 307–310, Jan. 2016, doi: 10.1016/j.procir.2016.02.053.

[14] M. Shabgard, S. Farzaneh, and A. Gholipoor, "Investigation of the surface integrity characteristics in wire electrical discharge machining of Inconel 617," *Journal of the Brazilian Society of Mechanical Sciences and Engineering*, vol. 39, no. 3, pp. 857–864, May 2016, doi: 10.1007/s40430-016-0556-0.

[15] P. Sharma, D. Chakradhar, and N. S, "Analysis and optimization of WEDM Performance Characteristics of Inconel 706 for aerospace application," *Silicon*, vol. 10, no. 3, pp. 921–930, Jul. 2017, doi: 10.1007/s12633-017-9549-6.

[16] M. P. Garg, A. Kumar, and C. K. Sahu, "Mathematical modeling and analysis of WEDM machining parameters of nickel-based super alloy using response surface methodology," *Sadhana*, vol. 42, no. 6, pp. 981–1005, Apr. 2017, doi: 10.1007/s12046-017-0647-3.

[17] P. Shandilya, H. Bisaria, and P. K. Jain, "Parametric study on the recast layer during EDWC of a Ni-rich NiTi shape memory alloy," *Journal of Micromanufacturing*, vol. 1, no. 2, pp. 134–141, May 2018, doi: 10.1177/2516598418766934.

[18] H. Bisaria and P. Shandilya, "Experimental investigation on wire electric discharge machining (WEDM) of Nimonic C-263 superalloy," *Materials and Manufacturing Processes*, vol. 34, no. 1, pp. 83–92, Dec. 2018, doi: 10.1080/10426914.2018.1532589.

[19] M. S. Rao and N. Venkaiah, "Experimental investigations on surface integrity issues of Inconel-690 during wire-cut electrical discharge machining process," *Proceedings of the Institution of Mechanical Engineers Part B Journal of Engineering Manufacture*, vol. 232, no. 4, pp. 731–741, Jun. 2016, doi: 10.1177/0954405416654092.

[20] P. S. Gowthaman and S. Jeyakumar, "A Review on machining of High Temperature Aeronautics Super-alloys using WEDM," *Materials Today Proceedings*, vol. 18, pp. 4782–4791, Jan. 2019, doi: 10.1016/j.matpr.2019.07.466.

[21] R. Joy, I. V. Manoj, and S. Narendranath, "Investigation of cutting speed, recast layer and micro-hardness in angular machining using slant type taper fixture by WEDM of Hastelloy X," *Materials Today Proceedings*, vol. 27, pp. 1943–1946, Oct. 2019, doi: 10.1016/j.matpr.2019.09.021.

[22] D. Srinivasan *et al.*, "Investigation on electric erosion behavior of nickel-based super alloy (Waspaloy: Ni, Cr, Co, Mo, Ti, Al) using response surface methodology," *Surface Topography Metrology and Properties*, vol. 9, no. 3, p. 035006, Jun. 2021, doi: 10.1088/2051-672x/ac0f33.

[23] L. W. Reolon, C. A. H. Laurindo, R. D. Torres, and F. L. Amorim, "WEDM performance and surface integrity of Inconel alloy IN718 with coated and uncoated wires," *The International Journal of Advanced Manufacturing Technology*, vol. 100, no. 5–8, pp. 1981–1991, Oct. 2018, doi: 10.1007/s00170-018-2828-6.

[24] O. C. Ozaner, G. Dursun, and G. Akbulut, "Effects of wire-EDM parameters on the surface integrity and mechanical characteristics of additively manufactured Inconel 939," *Materials Today Proceedings*, vol. 38, pp. 1861–1865, Sep. 2020, doi: 10.1016/j.matpr.2020.08.486.

[25] P. M. Abhilash and D. Chakradhar, "Surface integrity comparison of wire electric discharge machined Inconel 718 surfaces at different machining stabilities," *Procedia CIRP*, vol. 87, pp. 228–233, Jan. 2020, doi: 10.1016/j.procir.2020.02.037.

[26] Sudhir, A. K. Sehgal, and S. S. Nain, "Machine learning algorithms evaluation and optimization of WEDM of nickel based super alloy: A review," *Materials Today Proceedings*, vol. 50, pp. 1793–1798, Oct. 2021, doi: 10.1016/j.matpr.2021.09.202.

[27] C. Balasubramaniyan, K. Rajkumar, and S. Santosh, "Wire-EDM machinability investigation on quaternary Ni44Ti50Cu4Zr2 shape memory alloy," *Materials and Manufacturing Processes*, vol. 36, no. 10, pp. 1161–1170, Apr. 2021, doi: 10.1080/10426914.2021.1905833.

[28] A. G. Karthikeyan, K. Kalaiselvan, and N. Muralidharan, "CNC wire-cut EDM input variables analysis on Ni -based superalloy (MONEL K-500)," *Materials and Manufacturing Processes*, vol. 37, no. 9, pp. 1035–1044, Nov. 2021, doi: 10.1080/10426914.2021.2001522.

[29] K. Mouralova *et al.*, "Machining of B1914 nickel-based superalloy using wire electrical discharge machining," *Proceedings of the Institution of Mechanical Engineers Part E Journal of Process Mechanical Engineering*, vol. 235, no. 6, pp. 2141–2153, Jul. 2021, doi: 10.1177/09544089211031746.

[30] A. Polzer, K. Mouralova, L. Benes, R. Zahradnicek, and J. Fries, "Comparison of machinability of nickel alloys using WEDM," *Proceedings of the Institution of Mechanical Engineers Part B Journal of Engineering Manufacture*, vol. 236, no. 9, pp. 1268–1281, Feb. 2022, doi: 10.1177/09544054221075876.

[31] C. Devanathan, Natarajan, E. Shankar, R. Giri, and K. Vigneshwaran, "An effect of process parameters during wire cut electrical discharge machining of Inconel 738," *Materials Today Proceedings*, vol. 84, pp. 83–88, Jan. 2023, doi: 10.1016/j.matpr.2023.05.148.

[32] B. Alkahlan, T. Tabbakh, A. Kurdi, A. Pramanik, and A. K. Basak, "Formation and Characterization of the Recast Layer Formed on Inconel 718 during Wire Electro Discharge Machining," *Materials*, vol. 16, no. 3, p. 930, Jan. 2023, doi: 10.3390/ma16030930.

[33] S. Biswas, A. R. Paul, A. R. Dhar, Y. Singh, and M. Mukherjee, "Multi-material modeling for wire electro-discharge machining of Ni-based superalloys using hybrid neural network and stochastic optimization techniques," *CIRP Journal of Manufacturing Science and Technology*, vol. 41, pp. 350–364, Jan. 2023, doi: 10.1016/j.cirpj.2022.12.005.

[34] V. Karthikeyan, S. Rajesh, R. G. Padmanaban, A. J. Arockiam, and S. Sundaraselvan, "Processing and optimizing the wire EDM process parameters of SLM 3D-Printed UDimet Alloy 720," *Journal of Materials Engineering and Performance*, Sep. 2025, doi: 10.1007/s11665-025-12166-6.